

Observation of Resonant Quantum Magnetoelectric Effect in a Multiferroic Metal–Organic Framework

Ying Tian, Shipeng Shen, Junzhuang Cong, Liqin Yan, Shouguo Wang, and Young Sun*

State Key Laboratory of Magnetism, Institute of Physics, Chinese Academy of Sciences, Beijing 100190, PR China

S Supporting Information

ABSTRACT: A resonant quantum magnetoelectric coupling effect has been demonstrated in the multiferroic metal–organic framework of $[(\text{CH}_3)_2\text{NH}_2]\text{Fe}(\text{HCOO})_3$. This material shows a coexistence of a spin-canted antiferromagnetic order and ferroelectricity as well as clear magnetoelectric coupling below $T_N \approx 19$ K. In addition, a component of single-ion quantum magnets develops below ~ 8 K because of an intrinsic magnetic phase separation. The stair-shaped magnetic hysteresis loop at 2 K signals resonant quantum tunneling of magnetization. Meanwhile, the magnetic field dependence of dielectric permittivity exhibits sharp peaks just at the critical tunneling fields, evidencing the occurrence of resonant quantum magnetoelectric coupling effect. This resonant effect enables a simple electrical detection of quantum tunneling of magnetization.

In recent years, there has been remarkable interest in the synthesis and investigation of hybrid organic–inorganic materials, such as the metal–organic frameworks (MOFs), largely due to their potential applications in gas storage, catalysis, nonlinear optics, photoluminescence, and solar cells as well as their intriguing magnetic and electric properties for fundamental science study.^{1–6} In particular, MOFs with the ABX_3 perovskite-like structure are of great interest because the variable A and B components provide plenty of room for adjusting the physical and chemical properties in a simple crystalline structure. In 2009, Jain et al. reported multiferroic behavior in a family of perovskite MOFs,⁷ which stimulated considerable experimental and theoretical efforts to search for new multiferroic materials in hybrid MOFs.^{8–17} Multiferroic materials in which magnetic and electric orders coexist have been the subject of extensive research for more than a decade because of their promise for holding large magnetoelectric (ME) coupling effects, i.e., the mutual control of ferroelectric properties by magnetic fields and magnetism by electric fields.^{18–22}

Compared with inorganic multiferroic materials of transition metal oxides, the ME effects in multiferroic MOFs are very weak and even undetectable because their electric and magnetic orders usually have different origins. Only recently did our group first report clear ME effects in the multiferroic state of the perovskite MOF $[(\text{CH}_3)_2\text{NH}_2]\text{Fe}(\text{HCOO})_3$ (Fe-MOF).^{23,24} Moreover, we found that this Fe-MOF exhibits resonant quantum tunneling of magnetization (RQTM) at 2 K,²⁵ a phenomenon previously only seen in the single-molecule

and single-ion quantum magnets.^{26–29} Since the discovery of Mn_{12} single-molecular magnet, the RQTM has attracted remarkable research interests because of its potential for applications in information storage, quantum computing, and molecular spintronics. To measure the RQTM, sophisticated facilities such as superconducting quantum interference device (SQUID) or synchrotron-based spectroscopic techniques are usually employed to detect the magnetization tunneling.^{30,31}

The simultaneous presence of the RQTM and ME coupling makes this Fe-MOF very interesting and unique. In this communication, we demonstrate that the joint effects of the RQTM and ME coupling give rise to a resonant quantum ME effect at low temperatures. This completely new effect enables an electrical detection of RQTM in a very simple and efficient way.

We have prepared the Fe-MOF samples by a solvothermal condition method (details in the Supporting Information). Colorless single crystals with a maximum size of $2 \times 2 \times 2$ mm³ are obtained. Powder X-ray diffraction (XRD) at room temperature is performed to check the structure and phase purity of the synthesized samples. The XRD pattern (Figure S1) confirms that there is no secondary phase such as a mixed valence compound^{32,33} of Fe-MOF in our samples. The single-crystal XRD pattern suggests that the crystals are naturally grown layer by layer along [012] direction. As shown in Figure 1, the Fe-MOF has a perovskite-like ABX_3 structure. The metal cations ($\text{B} = \text{Fe}^{2+}$) linked by formate groups ($\text{X} = \text{HCOO}^-$) form the BX_3 skeleton and dimethylammonium (DMA) cations ($\text{A} = [(\text{CH}_3)_2\text{NH}_2]^+$) occupy the cavities. The amine hydrogen atoms of DMA⁺ form hydrogen bonds with the oxygen atoms of the formate groups.

The dielectric permittivity and magnetization along [012] direction of the Fe-MOF as a function of temperature are shown in Figure 2a,b, respectively. A paraelectric (PE) to ferroelectric (FE) phase transition is observed at $T_C \approx 164$ K, as evidenced by the sudden jump in the dielectric permittivity (Figure 2a). We also carried out pyroelectric current measurements and found a sharp pyroelectric peak at the dielectric phase transition, further confirming the ferroelectric ordering below $T_C \approx 164$ K (Figure S2). In addition, this perovskite MOF also exhibits magnetic ordering at low temperatures. As seen in Figure 2b, two magnetic transitions can be identified: one at $T_N \approx 19$ K and another around $T_B \approx 8$ K, below which the zero-field-cooled (ZFC) and field-cooled (FC) magnetization diverge. A careful study has suggested that there is a

Received: November 30, 2015

Published: January 8, 2016

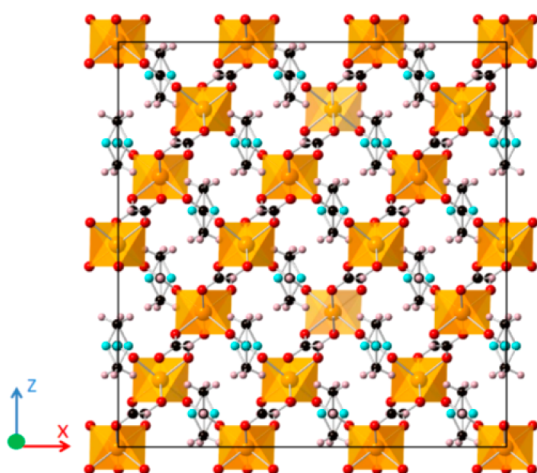


Figure 1. A side view of the perovskite-like structure of the metal-organic framework $[(\text{CH}_3)_2\text{NH}_2]\text{Fe}(\text{HCOO})_3$.

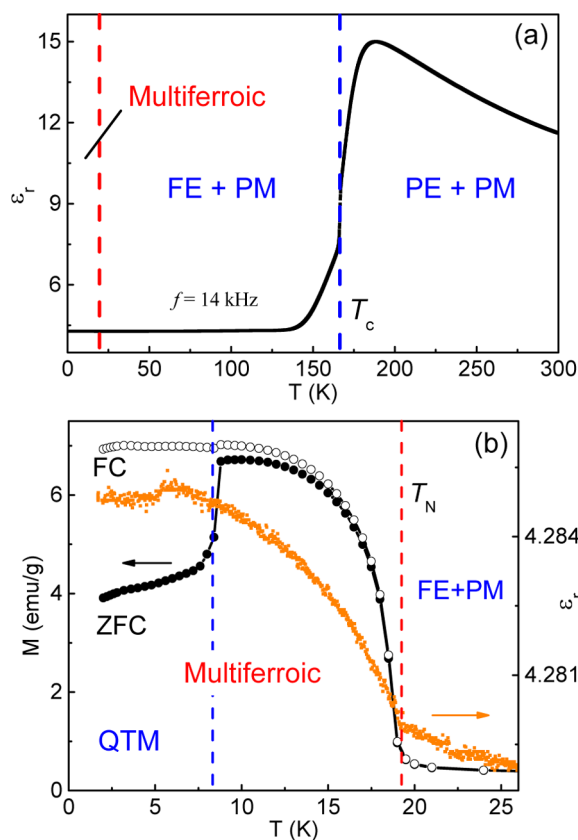


Figure 2. (a) Temperature dependence of dielectric permittivity. A paraelectric-ferroelectric (PE-FE) phase transition occurs at $T_c \approx 164$ K. (b) ZFC and FC magnetization in 0.1 T as a function of temperature. A paramagnetic (PM) to spin-canted antiferromagnetic transition occurs at $T_N \approx 19$ K. An anomaly in dielectric permittivity is observed at the magnetic ordering temperature.

magnetic phase separation in this perovskite Fe-MOF.²⁵ Accordingly, the sharp transition at T_N is due to the onset of a spin-canted antiferromagnetic (AFM) ordering, and the drop of the ZFC magnetization below T_B is due to the blocking of single-ion quantum magnets. Just at the magnetic ordering temperature T_N , the dielectric permittivity starts to increase rapidly as seen in Figure 2b. This coincidence between

magnetic ordering and dielectric anomaly is a strong evidence for ME coupling.^{34,35}

One unique feature of this Fe-MOF is that it exhibits RQTM at low temperatures. Figure 3a shows the M - H loop along

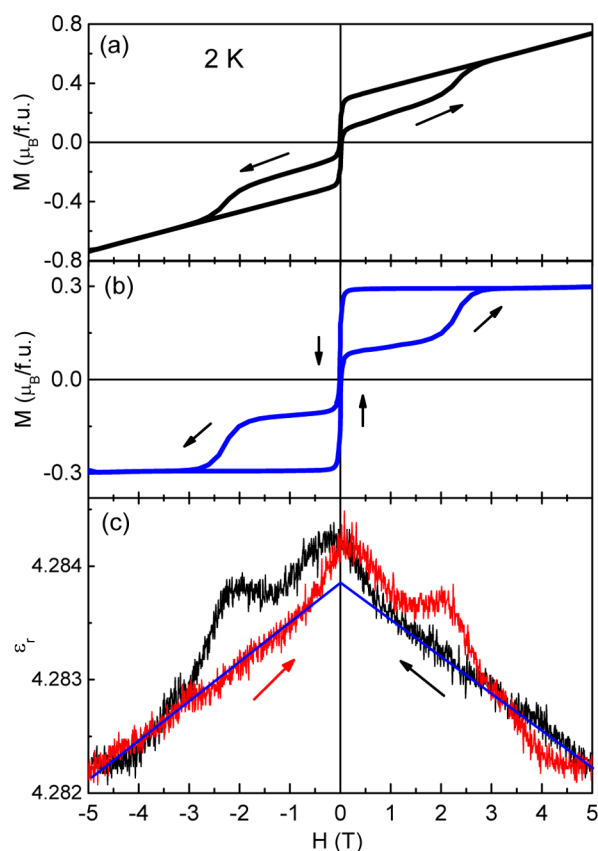


Figure 3. (a) M - H loop at 2 K. (b) Stair-shaped M - H loop after subtracting the linear $M(H)$ component at 2 K. (c) Dielectric permittivity as a function of scanning magnetic field at 2 K. The blue solid lines represent the linear dependences extrapolated to zero field.

[012] at 2 K. After subtracting the linear dependence of magnetization of the AFM component, we obtain a regular stair-shaped M - H loop shown in Figure 3b, which is a characteristic of RQTM.

The ME coupling in Fe-MOF is evidenced by the magnetodielectric effect at 2 K. As shown in Figure 3c, the dielectric permittivity decreases with increasing magnetic field. When comparing the magnetodielectric behavior with the M - H loop, we find an interesting correlation between them. At 2 K, the magnetization exhibits two sharp jumps at $H_1 = 0$ T and $H_2 = 2.2$ T or -2.2 T for the ascending and descending branch, respectively, corresponding to the occurrence of resonant tunneling of magnetization. The dielectric permittivity also shows two clear peaks at these critical fields, exactly matching with the RQTM. To confirm that the magnetodielectric behavior at 2 K is intrinsic, we also measured the magnetodielectric response at 15 K where the RQTM is absent. As seen in Figure S3, the dielectric permittivity at 15 K decreases monotonically with increasing magnetic field, unlike the behavior at 2 K.

The concurrence of the magnetodielectric peak and RQTM, termed as the resonant quantum ME effect, is more clearly illustrated in Figure 4, where the relative change of the dielectric permittivity ($\Delta\epsilon$) is compared with the differential of

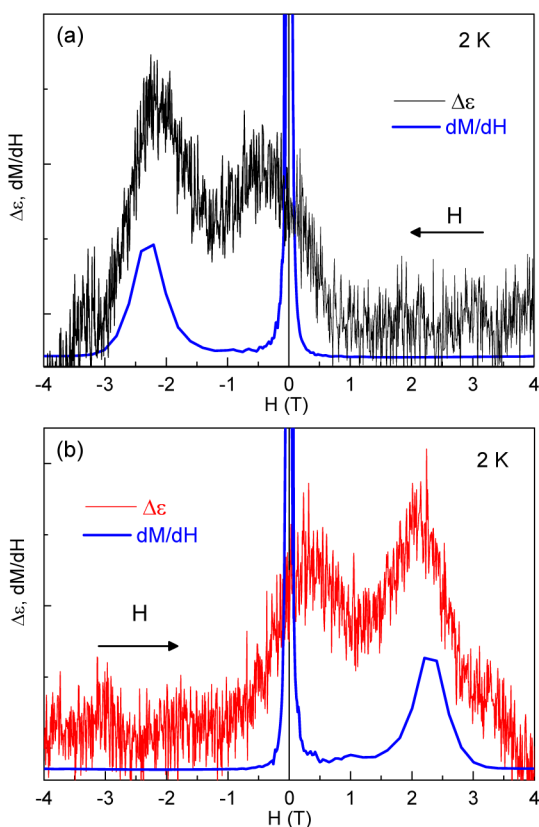


Figure 4. Comparison between the relative change of dielectric permittivity $\Delta\epsilon$ and the differential of magnetization dM/dH at 2 K for (a) descending magnetic field and (b) ascending magnetic field. The dielectric peaks appear at the same critical fields of RQTM, suggesting the resonant quantum magnetoelectric effects in the Fe-MOF.

magnetization (dM/dH) at 2 K. $\Delta\epsilon$ is obtained after subtracting the linear dependence of ϵ with H (blue solid lines in Figure 3c). When magnetic field is scanned from 5 to -5 T (Figure 4a), the dM/dH shows two sharp peaks at $H = 0$ and -2.2 T, corresponding to the positions of the RQTM. $\Delta\epsilon$ also exhibits sharp peaks at these positions. Similarly, when magnetic field is scanned from -5 to 5 T (Figure 4b), the RQTM occurs at $H = 0$ and 2.2 T, and $\Delta\epsilon$ also exhibits sharp peaks at these critical fields. Therefore, these results demonstrate that the RQTM can be clearly mapped by the magnetodielectric effect.

Below, we discuss the possible origin of this resonant ME effect. A systematic progression of contributions to the ME effects can be obtained from the expansion of the free energy:¹⁸

$$F(E, H) = F_0 - P_i^S E_i - M_i^S H_i - \frac{1}{2} \epsilon_0 \epsilon_{ij} E_i E_j - \frac{1}{2} \mu_0 \mu_{ij} H_i H_j - \alpha_{ij} E_i H_j - \frac{1}{2} \beta_{ijk} E_i H_j H_k - \frac{1}{2} \gamma_{ijk} H_i E_j E_k - \dots \quad (1)$$

where P^S and M^S are the spontaneous polarization and magnetization, α corresponds to the linear ME effect, and β and γ correspond to the higher-order ME effects. The differentiation of eq 1 gives

$$P_i(E, H) = -\frac{\partial F}{\partial E_i} = P_i^S + \epsilon_0 \epsilon_{ij} E_j + \alpha_{ij} H_j + \frac{1}{2} \beta_{ijk} H_j H_k + \gamma_{ijk} H_i E_j - \quad (2)$$

For the linear ME effect, the polarization is expected to vary linearly with applied magnetic field. Apparently, the linear ME effect alone is not able to account for the resonant ME effect in the Fe-MOF. High-order nonlinear ME effects have to play an important role. It is likely that both the A-group organic cations and the BX_3 framework are involved in the generation of polarization to give a dedicated ME coupling process.²³ Meanwhile, the tunneling of magnetization (magnetic moments) corresponds to a sudden change in angular momentum. Because of the conservation of the total angular momentum in the whole system, the surrounding lattice feels a transfer torque and induces an opposite change in phonon angular momentum, known as the Einstein–de Haas effect.³⁶ The spin–phonon interaction may give rise to a detectable change of the dielectric permittivity in response to the tunneling of magnetization.

In summary, we have demonstrated that the simultaneous presence of ME coupling and RQTM in the multiferroic Fe-MOF with a perovskite structure yields a novel resonant quantum ME effect. Along with the tunneling of magnetization, the dielectric permittivity exhibits sharp peaks due to the ME coupling. Thus, the quantum tunneling of magnetization can be simply detected by measuring the dielectric permittivity as a function of magnetic field.

■ ASSOCIATED CONTENT

Supporting Information

The Supporting Information is available free of charge on the ACS Publications website at DOI: 10.1021/jacs.5b12488.

Sample synthesis information, X-ray powder and single-crystal diffraction patterns, experimental details, pyroelectric and electric polarization data, and magnetodielectric effect at 15 K. (PDF)

Crystallographic information file for Fe-MOF. (CIF)

■ AUTHOR INFORMATION

Corresponding Author

*youngsun@iphy.ac.cn

Notes

The authors declare no competing financial interest.

■ ACKNOWLEDGMENTS

This work was supported by the Natural Science Foundation of China under grant nos. 11227405, 11534015, and 51371193 and the Chinese Academy of Sciences under grant nos. XDB07030200 and KJZD-EW-M05.

■ REFERENCES

- (1) Yaghi, O. M.; Li, G. M.; Li, H. L. *Nature* **1995**, 378, 703.
- (2) Kitagawa, S.; Kitaura, R.; Noro, S. *Angew. Chem., Int. Ed.* **2004**, 43, 2334.
- (3) Cheetham, A. K.; Rao, C. N. R. *Science* **2007**, 318, 58.
- (4) Wang, C.; Liu, D.; Lin, W. *J. Am. Chem. Soc.* **2013**, 135, 13222.
- (5) Li, W.; Gao, S.; Cheetham, A. K. *APL Mater.* **2014**, 2, 123801.
- (6) Shang, R.; Wang, Z.-M.; Gao, S. *Angew. Chem., Int. Ed.* **2015**, 54, 2534.

- (7) Jain, P.; Ramachandran, V.; Clark, R. J.; Zhou, H. D.; Toby, B. H.; Dalal, N. S.; Kroto, H. W.; Cheetham, A. K. *J. Am. Chem. Soc.* **2009**, *131*, 13625.
- (8) Rogez, G.; Viart, N.; Drillon, M. *Angew. Chem., Int. Ed.* **2010**, *49*, 1921.
- (9) Xu, G. C.; Zhang, W.; Ma, X. M.; Chen, Y. H.; Zhang, L.; Cai, H. L.; Wang, Z. M.; Xiong, R. G.; Gao, S. *J. Am. Chem. Soc.* **2011**, *133*, 14948.
- (10) Canadillas-Delgado, L.; Fabelo, O.; Rodriguez-Velamazan, J. A.; Lemee-Cailleau, M. H.; Mason, S. A.; Pardo, E.; Lloret, F.; Zhao, J. P.; Bu, X. H.; Simonet, V.; Colin, C. V.; Rodriguez-Carvajal, J. *J. Am. Chem. Soc.* **2012**, *134*, 19772.
- (11) Stroppa, A.; Jain, P.; Barone, P.; Marsman, M.; Perez-Mato, J. M.; Cheetham, A. K.; Kroto, H. W.; Picozzi, S. *Angew. Chem., Int. Ed.* **2011**, *50*, 5847.
- (12) Fu, D. W.; Zhang, W.; Cai, H. L.; Zhang, Y.; Ge, J. Z.; Xiong, R. G.; Huang, S. D.; Nakamura, T. *Angew. Chem., Int. Ed.* **2011**, *50*, 11947.
- (13) Pardo, E.; Train, C.; Liu, H. B.; Chamoreau, L. M.; Dkhil, B.; Boubekeur, K.; Lloret, F.; Nakatani, K.; Tokoro, H.; Ohkoshi, S.; Verdager, M. *Angew. Chem., Int. Ed.* **2012**, *51*, 8356.
- (14) Stroppa, A.; Barone, P.; Jain, P.; Perez-Mato, J. M.; Picozzi, S. *Adv. Mater.* **2013**, *25*, 2284.
- (15) Di Sante, D.; Stroppa, A.; Jain, P.; Picozzi, S. *J. Am. Chem. Soc.* **2013**, *135*, 18126.
- (16) Wang, W.; Yan, L. Q.; Cong, J. Z.; Zhao, Y. L.; Wang, F.; Shen, S. P.; Zou, T.; Zhang, D.; Wang, S. G.; Han, X. F.; Sun, Y. *Sci. Rep.* **2013**, *3*, 2024.
- (17) Tian, Y.; Stroppa, A.; Chai, Y.; Barone, P.; Perez-Mato, M.; Picozzi, S.; Sun, Y. *Phys. Status Solidi RRL* **2015**, *9*, 62.
- (18) Fiebig, M. *J. Phys. D: Appl. Phys.* **2005**, *38*, R123.
- (19) Eerenstein, W.; Mathur, N. D.; Scott, J. F. *Nature* **2006**, *442*, 759.
- (20) Cheong, S. W.; Mostovoy, M. *Nat. Mater.* **2007**, *6*, 13.
- (21) Spaldin, N. A.; Cheong, S. W.; Ramesh, R. *Phys. Today* **2010**, *63*, 38.
- (22) Sun, Y.; Yan, L. Q.; Cong, J. Z. *Sci. China: Phys., Mech. Astron.* **2013**, *56*, 222.
- (23) Tian, Y.; Stroppa, A.; Chai, Y.; Yan, L.; Wang, S.; Barone, P.; Picozzi, S.; Sun, Y. *Sci. Rep.* **2014**, *4*, 6062.
- (24) Tian, Y.; Cong, J.; Shen, S.; Chai, Y.; Yan, L.; Wang, S.; Sun, Y. *Phys. Status Solidi RRL* **2014**, *8*, 91.
- (25) Tian, Y.; Wang, W.; Chai, Y.; Cong, J.; Shen, S.; Yan, L.; Wang, S.; Han, X.; Sun, Y. *Phys. Rev. Lett.* **2014**, *112*, 017202.
- (26) Friedman, J. R.; Sarachik, M. P.; Tejada, J.; Ziolo, R. *Phys. Rev. Lett.* **1996**, *76*, 3830.
- (27) Wernsdorfer, W.; Sessoli, R. *Science* **1999**, *284*, 133.
- (28) Weng, D. F.; Wang, Z. M.; Gao, S. *Chem. Soc. Rev.* **2011**, *40*, 3157.
- (29) Jiang, S.-D.; Wang, B.-W.; Sun, H.-L.; Wang, Z.-M.; Gao, S. *J. Am. Chem. Soc.* **2011**, *133*, 4730.
- (30) Lorusso, G.; Sharples, J. W.; Palacios, E.; Roubeau, O.; Brechin, E. K.; Sessoli, R.; Rossin, A.; Tuna, F.; McInnes, E. J. L.; Collison, D.; Evangelisti, M. *Adv. Mater.* **2013**, *25*, 4653.
- (31) Mannini, M.; Pineider, F.; Danieli, C.; Totti, F.; Sorace, L.; Sainctavit, Ph.; Arrio, M.-A.; Otero, E.; Joly, L.; Cezar, J. C.; Cornia, A.; Sessoli, R. *Nature* **2010**, *468*, 417.
- (32) Hagen, K. S.; Naik, S. G.; Huynh, B. H.; Masello, A.; Christou, G. *J. Am. Chem. Soc.* **2009**, *131*, 7516.
- (33) Zhao, J.; Hu, B.; Lloret, F.; Tao, J.; Yang, Q.; Zhang, X.; Bu, X. *Inorg. Chem.* **2010**, *49*, 10390.
- (34) Kimura, T.; Goto, T.; Shintani, H.; Ishizaka, K.; Arima, T.; Tokura, Y. *Nature* **2003**, *426*, 55.
- (35) Hur, N.; Park, S.; Sharma, P. A.; Ahn, J. S.; Guha, S.; Cheong, S. *Nature* **2004**, *429*, 392.
- (36) Zhang, L.; Niu, Q. *Phys. Rev. Lett.* **2014**, *112*, 085503.